# Age-dependent nigral dopaminergic neurodegeneration and α-synuclein accumulation in RGS6-deficient mice

**Zili Luo,[1] Katelin E. Ahlers-Dannen,[1] Mackenzie M. Spicer,[1,2] Jianqi Yang,[1] Stephanie Alberico,[3] Hanna E. Stevens,[4] Nandakumar S. Narayanan,[5] and Rory A. Fisher[1]**

[1]Department of Pharmacology, University of Iowa Carver College of Medicine, Iowa City, Iowa, USA. [2]Interdisciplinary Graduate Program of Molecular Medicine, University of Iowa Carver College of Medicine, Iowa City, Iowa, USA. [3]Department of Neurology, New York University, New York, New York, USA. [4]Department of Psychiatry, University of Iowa Carver College of Medicine, Iowa City, Iowa, USA. [5]Department of Neurology, University of Iowa Carver College of Medicine, Iowa City, Iowa, USA.

**Parkinson's disease (PD) is primarily a nonfamilial, age-related disorder caused by α-synuclein accumulation and the progressive loss of dopamine neurons in the substantia nigra pars compacta (SNc). GPCR-cAMP signaling has been linked to a reduction in human PD incidence and α-synuclein expression. Neuronal cAMP levels are controlled by GPCRs coupled to $G_s$ or $G_{i/o}$, which increase or decrease cAMP, respectively. Regulator of G protein signaling 6 (RGS6) powerfully inhibits $G_{i/o}$ signaling. Therefore, we hypothesized that RGS6 suppresses $D_2$ autoreceptor-$G_{i/o}$ signaling in SNc dopamine neurons promoting neuronal survival and reducing α-synuclein expression. Here, we provide potentially novel evidence that RGS6 critically suppresses late-age-onset SNc dopamine neuron loss and α-synuclein accumulation. RGS6 is restrictively expressed in human SNc dopamine neurons and, despite their loss in PD, all surviving neurons express RGS6. $RGS6^{-/-}$ mice exhibit hyperactive $D_2$ autoreceptors with reduced cAMP signaling in SNc dopamine neurons. Importantly, $RGS6^{-/-}$ mice recapitulate key sporadic PD hallmarks, including SNc dopamine neuron loss, reduced nigrostriatal dopamine, motor deficits, and α-synuclein accumulation. To our knowledge, *Rgs6* is the only gene whose loss phenocopies these features of human PD. Therefore, RGS6 is a key regulator of $D_2$R-$G_{i/o}$ signaling in SNc dopamine neurons, protecting against PD neurodegeneration and α-synuclein accumulation.**

## Introduction

Parkinson's disease (PD) is the second most common neurodegenerative disorder after Alzheimer's disease (1). It is a devastating progressive neurological disorder characterized by the loss of dopamine (DA) neurons in the substantia nigra pars compacta (SNc) (2–4). These neurons project to the striatum and release DA to postsynaptic targets that control motor behavior. Thus, loss of these SNc DA neurons leads to the hallmark motor deficits associated with PD: bradykinesia, rigidity, and resting tremors. Identified genetic mutations account for 5%–9% of the risk of PD (1). A primary risk factor for PD is aging (5), with sporadic PD afflicting 2% of the population over 60 years of age and 15% over 85. Despite decades of research, the reason for the greater sensitivity of SNc DA neurons to degeneration and why their loss is strongly associated with aging in PD is unknown.

α-Synuclein aggregates in Lewy bodies are believed to play a crucial role in PD pathogenesis. In support of this hypothesis, human α-synuclein gene (*SNCA)* mutations as well as *SNCA* gene duplication dramatically increase the risk of early-onset PD (6–9). Furthermore, increased α-synuclein protein expression is observed in the aging human SNc (10, 11). Various mouse studies also speak to the critical role of α-synuclein in PD pathogenesis. Mice expressing mutant human α-synuclein (A53T) in CNS neurons are prone to profound neurodegeneration with characteristic histopathological features of PD as well as motor dysfunction (12). α-Synucleinopathy and motor defects are also observed in mice expressing WT human α-synuclein (13). Finally, striatal administration of synthetic misfolded mouse α-synuclein fibrils induces

**Conflict of interest:** The authors have declared that no conflict of interest exists.



**Submitted:** December 11, 2018
**Accepted:** May 16, 2019
**Published:** July 11, 2019.

**Reference information:** *JCI Insight*. 2019;4(13):e126769. https://doi.org/10.1172/jci.insight.126769.

SNc DA neuron degeneration and motor defects demonstrating cell-to-cell transmission of pathological α-synuclein in anatomically connected regions (14). Thus, having too much α-synuclein or its mutated forms can produce PD-like pathology in mice.

Recent studies have suggested a possible link between GPCR signaling, PD-associated neurodegeneration, and pathological α-synuclein accumulation. Mittal et al. (15) reported that β-agonists dramatically reduce both α-synuclein expression and the incidence of human PD as well as inhibit MPTP-induced SNc DA neuron loss in mice. These findings are intriguing given our recent discovery that regulator of G protein signaling 6 (RGS6) is required for SNc DA neuron survival in adult mice (16). RGS6 is a member of the RGS protein family, which is a critical modulator of GPCR signaling. Specifically, RGS proteins determine the magnitude and duration of GPCR signaling through their role as GTPase-activating proteins, allowing them to inactivate heterotrimeric G protein Gα subunits (17–19). In mice, we found that RGS6 is expressed in the same subset of SNc DA neurons that are lost in PD and that $RGS6^{-/-}$ mice consistently display SNc DA neuron degeneration beginning around 9 months. Furthermore, the expression of several DA $D_2$ autoreceptor ($D_2R$) targets is altered in SNc DA neurons of $RGS6^{-/-}$ mice (16), suggesting that RGS6-mediated attenuation of $D_2R$-$G_{i/o}$ signaling may be neuroprotective. Given that both β-agonists and RGS6 function to promote cAMP signaling by stimulating $G_s$ and inhibiting $G_{i/o}$ (20, 21), respectively, we hypothesized that RGS6 may promote SNc DA neuron survival by repressing pathological α-synuclein accumulation and resultant neurodegeneration.

Here, we demonstrate that RGS6 plays a critical role in preventing late-age-onset PD-associated neurodegeneration and pathological α-synuclein accumulation. First, we show that RGS6 is expressed in human SNc DA neurons that are lost with PD, consistent with what we have seen in mice. Second, RGS6 loss in mice results in a significant age-dependent reduction in SNc and striatal DA as well as impaired dopaminergic neurotransmission causing stereotypical PD motor deficits. Third, we show that RGS6 is absolutely required for regulation of $D_2R$ function, promoting proper DA synthesis and release, as well as SNc DA neuron survival. Finally, we provide evidence demonstrating that RGS6 functions to prevent pathological α-synuclein accumulation in aged mice. Together, these data identify RGS6 as a potentially novel and critical repressor of the $D_2R$ signaling involved in preventing both age-dependent PD-associated pathological α-synuclein expression and SNc DA neuron degeneration.

## Results

*RGS6 is expressed in human SNc DA neurons that are lost in PD and in aged $RGS6^{-/-}$ mice*. Our previous work in mice indicates that in the SNc, RGS6 is exclusively expressed in DA neurons (16). To determine whether this pattern of RGS6 expression is preserved in the human SNc, we performed an immunohistochemical analysis of RGS6 and tyrosine hydroxylase (TH) expression in human midbrain sections. Representative images of the paraffin-embedded midbrain tissue blocks containing the pigmented SNc DA neurons can be seen in Figure 1A. Immunohistochemical analysis of both control and PD specimens revealed that, as in mice, RGS6 is expressed in all DA ($TH^+$) neurons within the human SNc. Furthermore, an unbiased stereological analysis revealed that when compared with control SNc tissues, there is a significant 73% reduction in the density of both $TH^+$ and $RGS6^+$ neurons in the SNc of patients with PD (Figure 1A). This finding is similar to the 79% loss of $TH^+$ neurons in PD midbrains originally reported by Damier et al. (22). Thus, consistent with its proposed need for SNc DA neuron survival, RGS6 is expressed in all SNc DA neurons in humans, and all surviving neurons in patients with PD express RGS6. Immunohistochemical and unbiased stereological analysis of the mouse SNc revealed a 52% reduction in $TH^+$ neuron density in aged, 12-month-old $RGS6^{-/-}$ mice compared with $RGS6^{+/+}$ mice (Figure 1B). Thus, aged $RGS6^{-/-}$ mice exhibit robust SNc DA neuron loss, as seen in human PD. Further immunohistochemical analysis revealed that RGS6 is not only present in SNc DA neuron cell bodies, but is also expressed in DA terminals in the dorsal striatum (Supplemental Figure 1; supplemental material available online with this article; https://doi.org/10.1172/jci.insight.126769DS1).

*Aged $RGS6^{-/-}$ mice exhibit altered DA homeostasis and impaired motor performance*. RGS6 is expressed in SNc DA neurons and despite their loss in PD, all surviving neurons express RGS6. In addition, RGS6 deficiency in aged mice leads to loss of SNc DA neurons (Figure 1). These data suggest that RGS6 plays a crucial role in the function of these neurons and that losing RGS6 could result in altered DA content as well as impaired motor function due to loss of SNc DA neurons. To test this theory, we measured DA and its metabolites in the SNc and striatum of 3-, 9-, and 12-month-old $RGS6^{+/+}$ and $RGS6^{-/-}$ mice. In support of our hypothesis that RGS6 is critically involved in SNc DA neuron function, we found that with age, $RGS6^{-/-}$ mice exhibited a progressive and significant reduction in SNc and striatal DA content when com-

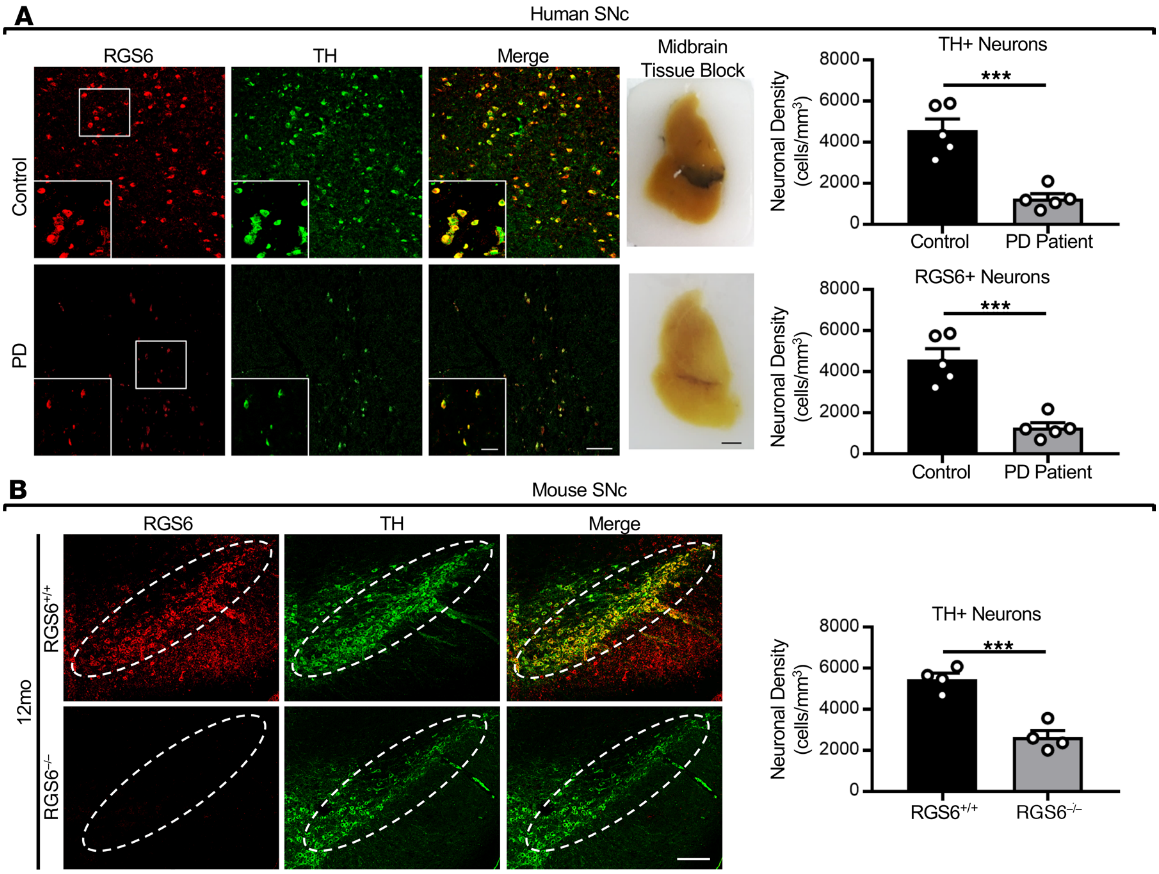


**Figure 1. RGS6 is exclusively expressed in dopaminergic TH⁺ neurons in the SNc of humans and mice, and these neurons are significantly reduced in humans with PD and RGS6-deficient mice.** (**A**) Left: Human SNc tissue sections derived from control and PD patient tissue blocks were stained with antibodies against RGS6 (red) and tyrosine hydroxylase (TH, green). Representative images of a control and PD specimen are shown here. The scale bar in the low-magnification confocal SNc images is 100 μm and 50 μm in the high-magnification insets. The scale bar for the tissue block images is 80 μm. Right: Unbiased stereological analysis of the prevalence of $TH^+$ and $RGS6^+$ cells within control and PD specimens demonstrates that there is a significant reduction in both $TH^+$ ($F_{crit}$ = 5.32, $P \leq 0.001$) and $RGS6^+$ ($F_{crit}$ = 5.32, $P \leq 0.001$) cells within the SNc of patients with PD when compared with that of controls. (**B**) Left: Immunostaining of SNc tissue sections from 12-month-old $RGS6^{+/+}$ and $RGS6^{-/-}$ mice for RGS6 and TH as in **A**. Right: Unbiased stereological analysis of $TH^+$ neurons within the SNc of 12-month-old $RGS6^{+/+}$ and $RGS6^{-/-}$ mice found a significant reduction in $TH^+$ neurons in $RGS6^{-/-}$ relative to $RGS6^{+/+}$ 12-month-old mice ($F_{crit}$ = 5.99, $P = 0.0007$). Data were analyzed using a 1-way ANOVA. Data are presented as the mean ± SEM ($n = 5$ per group in human control and PD patient tissue sections; $n = 4$ $RGS6^{+/+}$ and $RGS6^{-/-}$ mice). ***$P \leq 0.001$.

pared with their age-matched $RGS6^{+/+}$ controls. No significant reduction in striatal or SNc DA content was observed in $RGS6^{+/+}$ mice over this period (Figure 2, A and B). Remarkably, by 12 months of age, there was ≥50% reduction in DA content within the SNc and striatum of $RGS6^{-/-}$ mice.

Interestingly, DA levels were reduced in the striatum of $RGS6^{-/-}$ mice by 3 months, before any significant loss was detected in the SNc and before marked DA neuron degeneration occurs (16). This finding suggests that the loss of DA content in the striatum at 3 months is directly related to the ability of RGS6 to regulate DA synthesis and potentially its release, at the SNc dopaminergic axon terminal, where we found RGS6 is expressed robustly (Supplemental Figure 1). Further supporting a critical role of RGS6 in SNc DA handling, there was a significant increase in the 3,4-dihydroxyphenylacetic acid (DOPAC)/DA ratio in both the striatum and SNc of 12-month-old $RGS6^{-/-}$ mice relative to age-matched $RGS6^{+/+}$ mice (Figure 2, C and D). This is interesting as DOPAC, a major DA metabolite (23), has been shown to be increased relative to DA in the midbrains of humans with PD and is also associated with impaired vesicular DA uptake (24). Because DA in synaptic vesicles does not undergo metabolism to DOPAC, this observation suggests that RGS6 loss leads to DA accumulation in the cytoplasm and, given the overall decrease in DA content within the striatum, reduced synaptic DA. Taken together, these data provide potentially novel evidence of an age-dependent role for RGS6 in maintaining proper SNc DA homeostasis in mice.

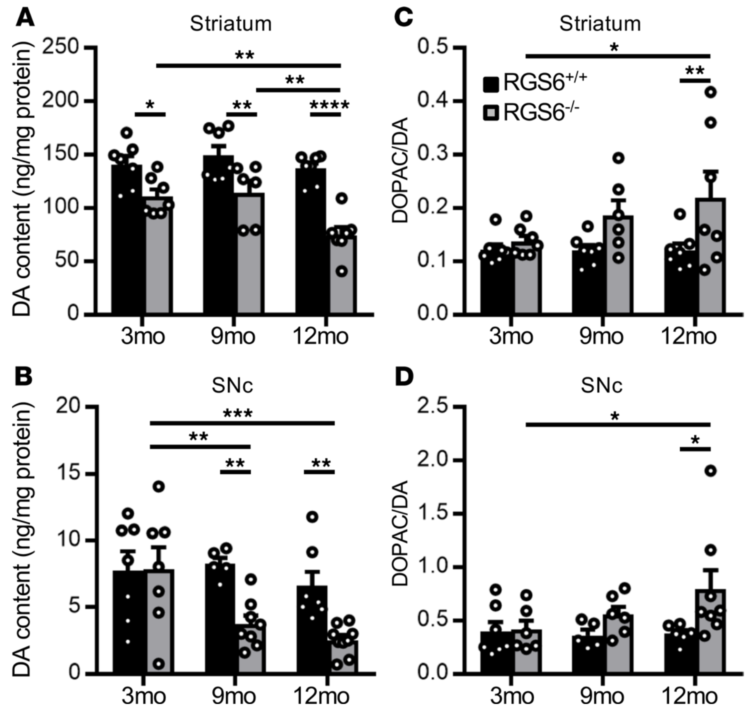


**Figure 2. RGS6 loss is associated with a significant age-dependent reduction in striatal and SNc DA levels and a concomitant increase in DOPAC/DA.** Levels of DA and its metabolites were measured in striatal and SNc tissues derived from 3-, 9-, and 12-month-old mice. (**A**) Striatal DA content was significantly decreased in RGS6$^{-/-}$ mice relative to RGS6$^{+/+}$ animals at every time point measured, and significant effects of both age [$F_{(2,35)}$ = 5.93, $P$ = 0.006] and strain [$F_{(1,35)}$ = 42.50, $P \leq 0.0001$] were observed. (**B**) SNc DA content was significantly reduced in RGS6$^{-/-}$ mice relative to RGS6$^{+/+}$ animals at 9 and 12 months. Significant effects of both age [$F_{(2,37)}$ = 5.04, $P$ = 0.012] and strain [$F_{(1,37)}$ = 10.88, $P$ = 0.002] were observed. (**C**) The striatal DOPAC/DA ratio was significantly increased in RGS6$^{-/-}$ mice relative to RGS6$^{+/+}$ animals at 12 months, and a significant effect of age was observed [$F_{(1,35)}$ = 8.97, $P$ = 0.005]. (**D**) The SNc DOPAC/DA ratio was also significantly increased in RGS6$^{-/-}$ mice relative to RGS6$^{+/+}$ animals at 12 months. As seen in the striatal DOPAC/DA ratio, a significant effect of age was also observed in the SNc [$F_{(1,32)}$ = 4.91, $P$ = 0.034]. Data were analyzed using a 2-way ANOVA with Fisher LDS post hoc adjustment. Data are presented as mean ± SEM ($N$ = 5–7 RGS6$^{+/+}$ mice and 6–9 RGS6$^{-/-}$ mice). $^*P \leq 0.05$, $^{**}P \leq 0.01$, $^{***}P \leq 0.001$, $^{****}P \leq 0.0001$.

SNc DA neurons powerfully regulate movement. As such, we hypothesized that the degeneration of SNc DA neurons in aged RGS6$^{-/-}$ mice would cause PD-associated motor deficits, which we investigated via a variety of assays. First, we found that 12-month-old RGS6$^{-/-}$ mice have impaired rotarod performance, exemplified by a significantly decreased latency to fall, in comparison with age-matched RGS6$^{+/+}$ controls (Figure 3A). Previously, we showed that young (3-month-old) RGS6$^{-/-}$ mice had GABA$_B$R-dependent rotarod and forelimb gait deficits due to excessive cerebellar GABA signaling that were reversed by a GABA$_B$R antagonist. However, the impaired rotarod performance of aged (12-month-old) RGS6$^{-/-}$ mice was not reversed by GABA$_B$R antagonist SCH-50911 but rather was partially reversed by L-3,4-dihydroxyphenylalanine (L-DOPA), confirming that the motor deficits seen in 12-month-old RGS6$^{-/-}$ mice are the direct result of reduced dopaminergic signaling (Figure 3A). Aged RGS6$^{-/-}$ animals also had deficits in open-field locomotion (Figure 3B), in contrast to increased open-field activity of 3-month-old RGS6$^{-/-}$ mice compared with RGS6$^{+/+}$ controls (ref. 25; see below). To further quantify movement, we turned to DigiGait, which measures gait dynamics using an automated treadmill gait test. Aged RGS6$^{-/-}$ mice showed a decrease in hind limb stride length and an increase in hind limb stride frequency that could be partially reversed, once again, through treatment with L-DOPA, but not SCH-50911 (Figure 3, C and D). Interestingly, the movement disorders reported here for RGS6$^{-/-}$ mice are seen in aged but not young mice (25, 26) and are characteristic of other mouse models of PD (27–36). Taken together, these data demonstrate that RGS6$^{-/-}$ mice not only display age-dependent loss of SNc DA neurons but also the accompanying PD-like motor dysfunction.

*RGS6 loss leads to increased $D_2R$ signaling in SNc DA neurons*. $G_{i/o}$-coupled $D_2$Rs negatively regulate DA neurotransmission by inhibiting DA synthesis and release while concomitantly promoting DA reuptake into the presynaptic terminal (37–40). Specifically, $D_2$R activation inhibits TH phosphorylation and activation

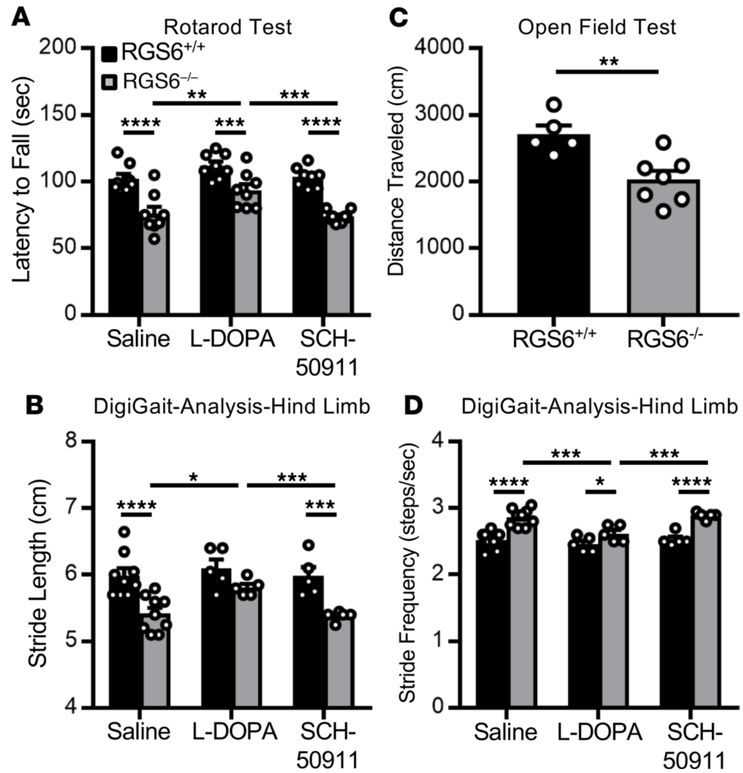


**Figure 3. RGS6$^{-/-}$ mice exhibit late-age-onset motor impairments that can be partially reversed by L-DOPA treatment.** (**A**) Rotarod test: When compared with age-matched RGS6$^{+/+}$ controls, 12-month-old RGS6$^{-/-}$ mice treated with saline displayed a significantly reduced latency to fall. The impaired rotarod performance was partially reversed by L-DOPA but not the $GABA_B$R antagonist SCH-50991. Significant effects of both strain [$F_{(2,42)} = 9.01$, $P = 0.01$] and treatment [$F_{(1,42)} = 65.36$, $P \leq 0.0001$] were observed ($N = 8$ RGS6$^{+/+}$ and RGS6$^{-/-}$ mice/treatment group). (**B**) Open-field test: 12-month-old RGS6$^{-/-}$ mice traveled a significantly shorter total distance than age-matched RGS6$^{+/+}$ controls ($F_{crit} = 4.96$, $P = 0.0054$) ($N = 5$ RGS6$^{+/+}$ and 7 RGS6$^{-/-}$ mice). (**C** and **D**) Automated treadmill gait test: Twelve-month-old RGS6$^{-/-}$ mice had a significantly shortened hind limb stride length (**C**) and an elevated hind limb stride frequency compared with age-matched RGS6$^{+/+}$ controls (**D**). Both gait abnormalities were partially reversed by L-DOPA treatment. Significant effects on both treatment and strain were observed in hind limb stride length [treatment: $F_{(2,32)} = 3.58$, $P = 0.039$; strain: $F_{(1,32)} = 29.86$, $P \leq 0.0001$] and frequency [treatment: $F_{(2,32)} = 7.00$, $P = 0.003$; strain: $F_{(1,32)} = 52.47$, $P \leq 0.0001$]. Data were analyzed using a 2-way ANOVA with the Fisher LSD post hoc adjustment (**A**, **C**, and **D**) or with a 1-way ANOVA (**B**). Data are presented as mean ± SEM ($n$ = 5–9 RGS6$^{+/+}$ and RGS6$^{-/-}$ mice/treatment group). *$P \leq 0.05$, **$P \leq 0.01$, ***$P \leq 0.001$.

through inhibition of adenylyl cyclase, inhibits the probability of DA release by activating $K^+$ and inhibiting $Ca^{2+}$ channels, and increases the plasma membrane expression of dopamine transporter (DAT). Given our findings that RGS6 plays a critical role in negatively regulating signaling by various $G_{i/o}$-coupled receptors in vivo (25, 26, 41) and that degeneration of SNc DA neurons in aged RGS6$^{-/-}$ mice is associated with increased DAT expression (16), we hypothesized that RGS6 suppresses $D_2$R-$G_{i/o}$–mediated inhibition of DA synthesis and release. To test this hypothesis, we evaluated the effects of the $D_2$R agonist quinpirole on the suppression of locomotion in 3-month-old RGS6$^{+/+}$ and RGS6$^{-/-}$ mice. Young mice were used in this study to avoid the late-age-onset SNc neurodegeneration resulting from RGS6 deficiency. Numerous studies have shown that quinpirole suppression of locomotion in mice is due to its presynaptic actions on activating the $D_2$R in the nigrostriatal pathway (42–45). These studies demonstrated that mice lacking presynaptic but not postsynaptic $D_2$Rs lose quinpirole suppression of locomotion as well as quinpirole inhibition of firing and DA release, both measures of presynaptic $D_2$R function, from SNc DA neurons. As shown in Figure 4, although 3-month-old RGS6$^{-/-}$ mice have a modest increase in locomotor activity compared with RGS6$^{+/+}$ mice as we previously reported (25), they are significantly more sensitive to quinpirole-locomotor suppression as measured by total distance traveled (Figure 4A), open-field velocity (Figure 4B), and movement to center (Figure 4C). Both the overall effect of quinpirole on these locomotor measures and their change from saline-treated mice was significantly greater (50%–100% greater) in RGS6$^{-/-}$ mice compared with RGS6$^{+/+}$ mice. For example, quinpirole reduced the distance traveled, velocity, and moving to center by 79%, 79%, and 59%, respectively,

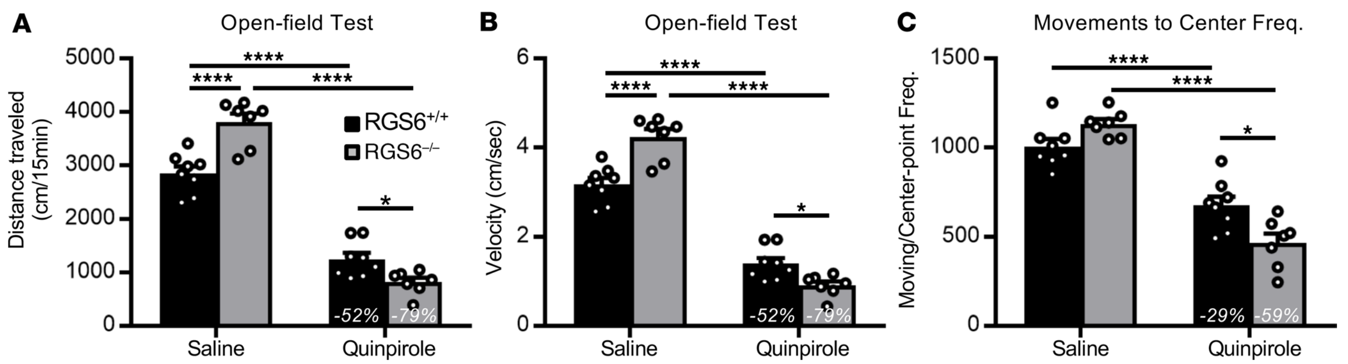


**Figure 4. RGS6$^{-/-}$ mice show increased sensitivity to quinpirole suppression of locomotion compared with RGS6$^{+/+}$ control mice.** Locomotor activity was quantified by measuring (**A**) distance traveled, (**B**) travel velocity, as well as (**C**) frequency of movements to center of RGS6$^{+/+}$ and RGS6$^{-/-}$ mice for 15 minutes following i.p. injection with either saline or quinpirole. Overall, quinpirole's ability to suppress locomotion was significantly greater in 3-month-old RGS6$^{-/-}$ mice compared with RGS6$^{+/+}$ mice (**A**) Significant effects of treatment [$F_{(1,25)} = 311.16$, $P \leq 0.0001$], strain [$F_{(1,25)} = 5.38$, $P = 0.029$], and interaction [$F_{(1,25)} = 26.28$, $P \leq 0.0001$] were observed in distance traveled by the mice. (**B**) Significant effects of treatment [$F_{(1,26)} = 327.69$, $P \leq 0.0001$] and interaction [$F_{(1,26)} = 30.33$, $P \leq 0.0001$] were found in mouse travel velocity. (**C**) Significant effects of treatment [$F_{(1,26)} = 125.14$, $P \leq 0.0001$] and interaction [$F_{(1,26)} = 14.20$, $P = 0.001$] were found in mouse movement to center frequency. Data were analyzed using 2-way ANOVAs with Fisher LSD post hoc analysis. Data are presented as mean ± SEM ($n$ = 8 saline RGS6$^{+/+}$; 7 saline RGS6$^{-/-}$ mice; 8 quinpirole RGS6$^{+/+}$ mice; 6–7 quinpirole RGS6$^{-/-}$ mice). *$P \leq 0.05$, **$P \leq 0.01$, ***$P \leq 0.001$, ****$P \leq 0.0001$.

in RGS6$^{-/-}$ mice and by 52%, 52%, and 29%, respectively in RGS6$^{+/+}$ mice. These findings provide in vivo evidence that RGS6 functions to suppress $D_2$R-mediated $G_{i/o}$ signaling in DA neurons.

*RGS6 loss leads to aberrant α-synuclein accumulation*. Given the ability of RGS6 to promote cAMP accumulation in the SNc through its inhibition of $G_{i/o}$ (20, 21), we hypothesized that RGS6 may suppress α-synuclein expression as other cAMP-elevating agents, such as β-agonists (15) have been recently reported to do. To test our hypothesis, we performed an immunohistochemical analysis of α-synuclein and TH expression in the SNc of 3-, 12-, and 18-month-old RGS6$^{+/+}$ and RGS6$^{-/-}$ mice. As shown in Figure 5, A and B, RGS6$^{-/-}$ mice exhibited not only age-dependent SNc DA neuron loss at 12 and 18 months, but also a concomitant and dramatic increase in α-synuclein expression compared with RGS6$^{+/+}$ mice or 3-month-old mice of either genotype. The increase in α-synuclein expression was more pronounced at 18 months than 12 months. Interestingly, and unlike what was seen in 3-month-old mice of either genotype as well as aged RGS6$^{+/+}$ mice, most of the α-synuclein in the SNc of 12- and 18-month-old RGS6$^{-/-}$ mice was not colocalized with DA neurons and was instead found extracellularly (Figure 5C). This finding was confirmed through quantitative comparison of the relative localization of α-synuclein with TH, an intracellular marker of DA neurons. Both intracellular and extracellular oligomeric forms of α-synuclein are linked to PD pathophysiology (46–48). Following SDS PAGE and immunoblotting, these α-synuclein oligomers appear as distinct higher-molecular-weight forms of the protein or protein smears. In brains or spinal cords derived from transgenic mice expressing PD-causing human α-synuclein mutants or those with intracerebral injections of α-synuclein fibrils, α-synuclein oligomers are found in nonionic detergent-insoluble, SDS- or urea-soluble fractions (12, 14, 49, 50). Alternatively, these oligomeric forms of α-synuclein can also be visualized in whole-brain homogenates derived from transgenic mice expressing mutant human α-synuclein and leucine-rich repeat kinase 2–deficient mice (51, 52). Utilizing the whole RIPA homogenate method of α-synuclein detection described by Giaime et al. (52), in Figure 5, D and E, we show that there is significantly greater oligomeric (higher-molecular-weight [HMW]) α-synuclein immunoreactivity in SNc punches derived from 12-month-old RGS6$^{-/-}$ mice relative to RGS6$^{+/+}$ controls. These data are consistent with our immunohistochemical findings in Figure 5, A–C. Together, these findings show that the late-age-onset dopaminergic neurodegeneration observed in the SNc of RGS6$^{-/-}$ mice is accompanied by aberrant α-synuclein accumulation.

*cAMP signaling is attenuated in RGS6$^{-/-}$ SNc DA neurons*. We sought to investigate whether RGS6 loss leads to decreased cAMP-PKA signaling in SNc DA neurons. This possibility is suggested both by our finding that RGS6 loss increases $G_{i/o}$-coupled $D_2$R activity in SNc DA neurons (Figure 4) as well as our discovery that RGS6 loss causes increased SNc α-synuclein accumulation (Figure 5) — the latter suppressed by cAMP-elevating β-agonists (15). As predicted, the data shown in Figure 6, A and B, demonstrate that RGS6 loss leads to a significant reduction in PKA activity in SNc DA neurons by 12 months, as measured

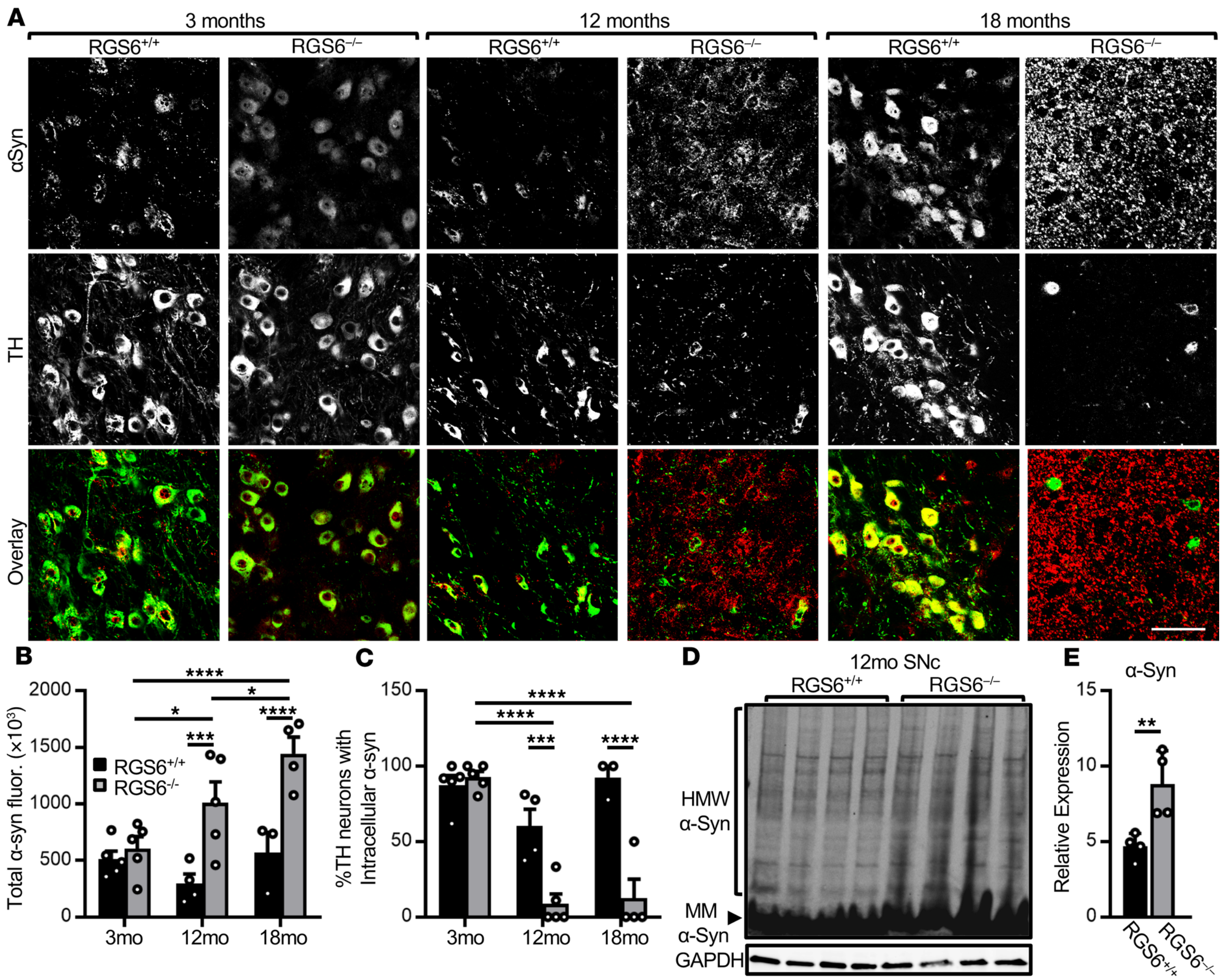


**Figure 5. RGS6$^{-/-}$ mice display increased expression of pathological α-synuclein accumulation relative to RGS6$^{+/+}$ control mice.** (**A**) IHC staining of α-synuclein (red) and TH (green) of DA neurons in the SNc of 3-, 12-, and 18-month-old RGS6$^{+/+}$ and RGS6$^{-/-}$ mice ($n$ = 3–5 mice/group). Scale bar: 40 μm. (**B** and **C**) Quantification of staining comparing corrected total α-synuclein fluorescence (**B**) and the number of RGS6$^{+}$/TH$^{+}$ neurons containing intracellular α-synuclein (**C**) in RGS6$^{+/+}$ and RGS6$^{-/-}$ mice at 3, 12, and 18 months of age. A significant effect of strain was observed in both (**C**) [$F_{(1,12)}$ = 23.37, $P$ = 0.000] and (**D**) [$F_{(1,24)}$ = 44.01, $P \leq 0.0001$] ($n$ = 4–5 RGS6$^{+/+}$ and RGS6$^{-/-}$ mice/age group). (**D** and **E**) Western blotting (**D**) and quantification (**E**) of α-synuclein collected from SNc tissues of 12-month-old RGS6$^{+/+}$ and RGS6$^{-/-}$ mice ($n$ = 4 mice/group) using the Syn-1 antibody, with GAPDH as a loading control. Increased expression of α-synuclein is characterized by an aberrant smearing pattern, as observed in RGS6$^{-/-}$ but not WT mice. Data were analyzed using either 1- (**E**) or 2-way (**B** and **C**) ANOVA with Fisher LSD post hoc analysis. Data are presented as mean ± SEM. $^{**}P \leq 0.01$, $^{***}P \leq 0.001$.

using an antibody recognizing the phosphorylated PKA substrate motif. Similarly, TH phosphorylation at S40 mediated by cAMP-PKA, was also significantly decreased in RGS6$^{-/-}$ mice at 12 months (Figure 6, C and D). Importantly, this reduction in pS40 TH levels in 12-month-old RGS6$^{-/-}$ mice could be reversed through treatment of mice with either the $D_2R$ antagonist raclopride (3 mg/kg) or the activator of adenylyl cyclase forskolin (3.75 mg/kg; Figure 6, E and F). These results confirm that the canonical function of RGS6 to inhibit $D_2R$-$G_{i/o}$ signaling promotes cAMP-PKA signaling in SNc DA neurons.

In keeping with its role in modulating $D_2R$-$G_{i/o}$ signaling in SNc DA neurons, RGS6 exhibits a predominant membrane/cytosolic localization in these neurons (Supplemental Figure 2). Loss of RGS6 did not alter the expression of other R7 members in the SNc or striatum (Supplemental Figure 3).

## Discussion

The results depicted herein show that RGS6-deficient mice remarkably recapitulated the late-age-onset loss of SNc DA neurons (ref. 16 and Figure 1), DA loss (Figure 2), motor dysfunction (Figure 3), and aberrant expression of α-synuclein (Figure 5) characteristic of the majority of patients with PD. To our knowledge,

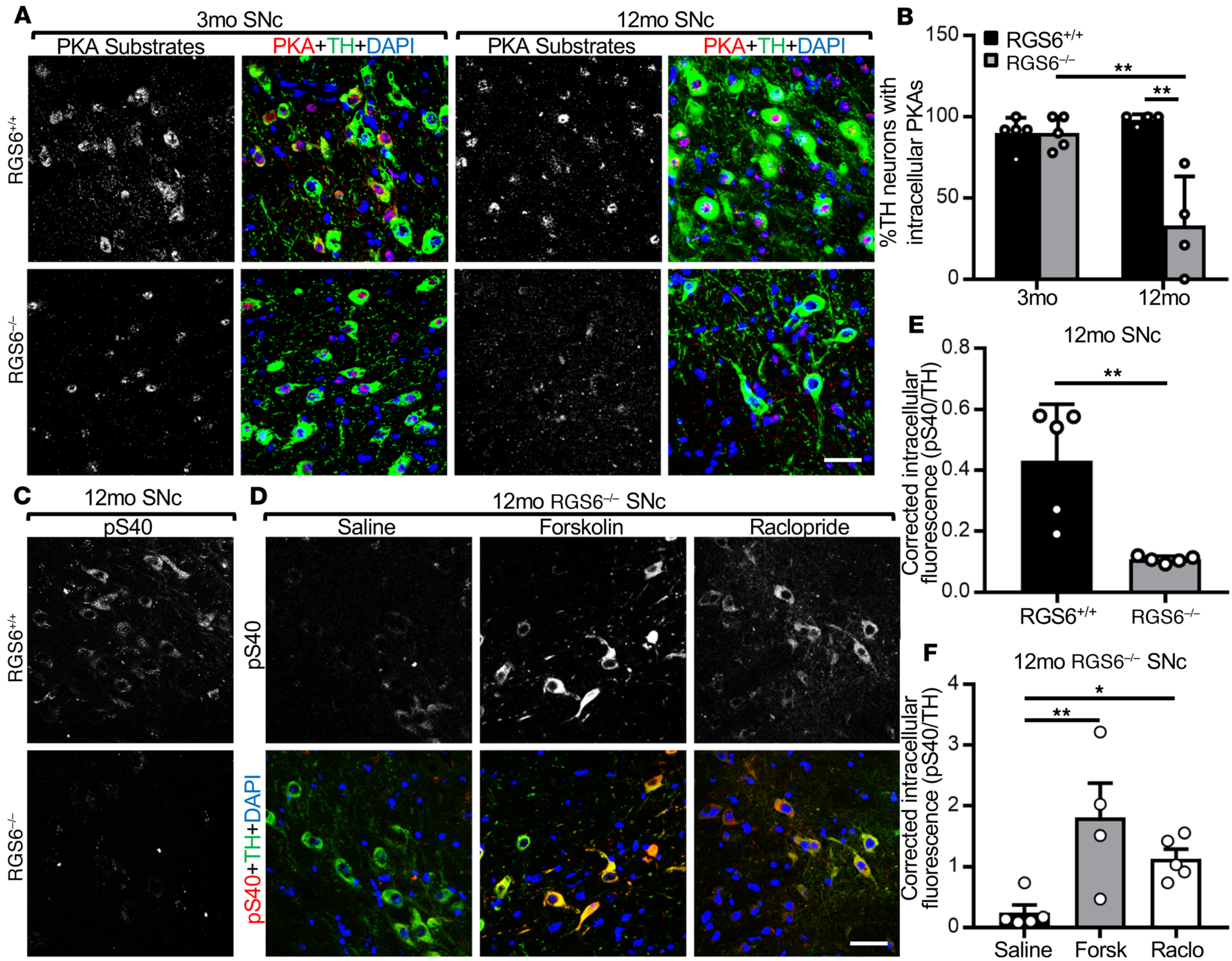


**Figure 6. RGS6 loss results in increased $D_2$R-$G_{i/o}$ signaling in SNc DA neurons in mice at 12 months.** (**A**) Representative IHC staining of PKAs (red), TH (green), and DAPI (blue) of DA neurons in the SNc of 3- and 12-month-old RGS6$^{+/+}$ and RGS6$^{-/-}$ mice. Scale bar: 25 μm. (**B**) Quantification of staining comparing percent of TH$^+$ neurons containing intracellular PKA-phosphorylated substrates in RGS6$^{+/+}$ and RGS6$^{-/-}$ mice at 3 and 12 months of age. Significant effects of age [$F_{(1,14)}$ = 93.97; $P < 0.0001$], strain [$F_{(1,14)}$ = 23.81; $P$ = 0.00], and interaction [$F_{(1,14)}$ = 23.82; $P$ = 0.00] were observed ($N$ = 4 mice per group). (**C**) Representative IHC staining of pS40 TH (red), TH (green), and DAPI (blue) of DA neurons in the SNc of 12-month-old RGS6$^{+/+}$ and RGS6$^{-/-}$ mice and in (**D**) 12 month-old RGS6$^{-/-}$ mice treated with vehicle (saline), forskolin (3.75 mg/kg, 45 minutes), or raclopride (3 mg/kg, 30 minutes). (**E**) Quantification of staining comparing intracellular pS40 TH levels in SNc DA neurons in 12-month-old RGS6$^{+/+}$ and RGS6$^{-/-}$ mice reveals a significant effect of strain ($n$ = 5 mice/group; $F_{crit}$ = 15.18; $P$ = 0.005). (**F**) Quantification of staining comparing intracellular pS40 TH levels in SNc DA neurons in 12-month-old RGS6$^{-/-}$ mice treated with vehicle (saline), forskolin, or raclopride as described in (**D**). A significant effect of treatment was observed ($n$ = 4–5 mice/treatment group; $F_{crit}$ = 6.47; $P$ = 0.014). Data were analyzed using either 1- (**E** and **F**) or 2-way (**B**) ANOVA analyses. Data are presented as mean ± SEM. *$P \le 0.05$, **$P \le 0.01$.

*RGS6* is the only known gene whose loss phenocopies these features of sporadic PD, thus identifying RGS6 as a disease-relevant target for PD treatment. In addition, we show that RGS6 is a key negative modulator of $G_{i/o}$ signaling in SNc DA neurons, with its loss provoking enhanced $D_2$R activity and a subsequent reduction in cAMP-PKA signaling (Figures 4 and 6). The ability of RGS6 to promote cAMP-PKA signaling may contribute to its neuroprotective functions and its ability to suppress α-synuclein expression. cAMP-PKA signaling has been shown to be neuroprotective in mouse models of PD (53–55), and cAMP-elevating β-agonists both reduce the incidence of human PD and suppress SNc α-synuclein expression in humans and mice (15). Furthermore, RGS6 is expressed in human SNc DA neurons and is lost with these DA neurons in patients with PD. Importantly, all surviving SNc DA neurons in patients with PD express RGS6. Together, these findings have guided us to the hypothesis that RGS6, through its canonical function in GPCR signaling (in this case, $D_2$R signaling) is required for SNc DA neuron survival and function (Figure 7). This insight has the potential to spur a new direction of research for the understanding of PD and its treatment.

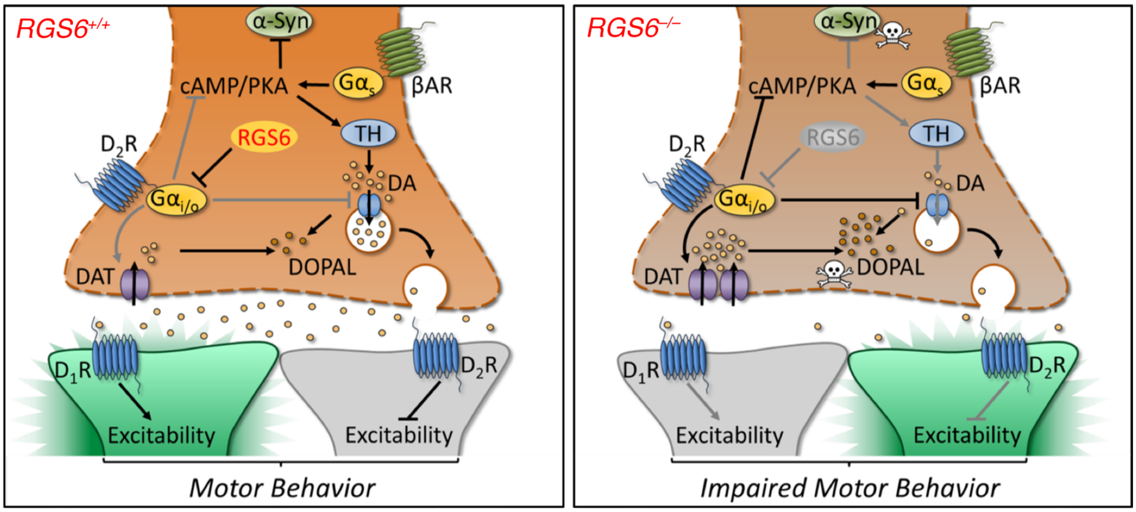


**Figure 7. The proposed role of RGS6 in the regulation of presynaptic $D_2$ receptor signaling in SNc DA neurons.** $G_{i/o}$-coupled $D_2$Rs expressed presynaptically on DA neurons (Supplemental Figure 1) act as autoreceptors inhibiting DA synthesis and vesicular DA release as well as upregulating DAT though multiple mechanisms (37–40, 79). Left: Our data indicated that, by serving as a gatekeeper for $D_2$R-$G_{i/o}$ signaling in SNc DA neurons, RGS6 ensures normal DA homeostasis and neurotransmission as well as suppresses aberrant accumulation of α-synuclein. By inhibiting $D_2$R-$G_{i/o}$ signaling, RGS6 promotes cAMP-PKA signaling, which increases DA synthesis (by TH phosphorylation) and suppresses α-synuclein expression similarly to cAMP-elevating β-agonists. RGS6 also promotes normal DA packaging and release by inhibiting $D_2$R-$G_{i/o}$–mediated inhibition of VMAT2 as well as upregulation/activation of DAT. Right: Loss of RGS6 disinhibits $D_2$R-$G_{i/o}$ signaling, which reduces cAMP and its effects on DA synthesis as well as α-synuclein accumulation, while simultaneously leading to accumulation of cytotoxic DA by $D_2$R-$G_{i/o}$-mediated inhibition of VMAT2 and upregulation of DAT.

The particular relevance of the RGS6$^{-/-}$ mouse for human PD lies not only in its ability to recapitulate the stereotypical late-age-onset death of SNc DA neurons, but also in its ability to reproduce deficits in DA synthesis, release, and catabolism that have been described in other animal models (56, 57). We found that concomitant with SNc DA neuron degeneration in RGS6$^{-/-}$ mice, there is a significant age-dependent reduction in DA content within the SNc and striatum (Figure 2). This reduction in striatal DA content is also seen in mouse models where G$\beta_5$, an atypical Gβ subunit that stabilizes R7 family members (RGS6, 7, 9, and 11; refs. 20, 58, 59), is genetically ablated (60).

A point of interest in the RGS6$^{-/-}$ mouse model is that the significant reduction in DA begins in the striatum as early as 3 months (Figure 2A), well before neurodegeneration is seen in these animals (16). These data suggest that the reduction in DA content is not solely due to neuronal loss, but that RGS6 itself is potentially responsible for proper DA synthesis, catabolism, release, and reuptake in the nigrostriatal pathway. This supposition is consistent with our previous findings demonstrating that RGS6-deficient SNc neurons display altered expression of several proteins that are required for DA synthesis, packaging, and uptake (16). Specifically, we found that RGS6-deficient SNc neurons have reduced levels of TH and vesicular monoamine transporter 2 (Vmat2) and an increase in DAT expression (16). Thus, despite having an impaired ability to synthesize DA (low TH) these RGS6-deficient neurons would be predicted to have abnormally high levels of cytosolic DA due to their inability to properly package the DA into vesicles (low Vmat2) and an accelerated rate of DA reuptake from the synaptic cleft (high DAT; refs. 61). In agreement with this prediction, we demonstrate that at 12 months, the DOPAC/DA ratio was significantly increased in both the striatum and SNc of RGS6$^{-/-}$ mice (Figure 2, C and D). Because DA metabolism occurs in the cytoplasm, these data demonstrate an impaired ability of RGS6-deficient SNc DA neurons to properly manage DA packaging and transmission. Our results recapitulate a similar increase in the DOPAC/DA ratio seen not only in other animal PD models but also in human PD patient samples (24, 62–65). Additionally, alterations in the expression of VMAT2, DAT, and ALDH1A within the SNc of RGS6$^{-/-}$ mice may reveal the toxic mechanism responsible for SNc DA neuron degeneration, as previous studies using transgenic mice have demonstrated that while VMAT2 and ALDH1A protect SNc DA neurons and oppose PD, increases in DAT expression provoke SNc neurodegeneration (66–71). Exactly how alteration in these factors lead to neurodegeneration is uncertain, but it is possible that the dysfunction in the transportation, storage, and catabolism of DA caused by their altered expression may contribute to an accumulation of cytotoxic DA metabolites, such as 3,4-dihydroxyphenylacetaldehyde in the cytosol (Figure 7 and refs. 72–76).

The ability of RGS6 to modulate the expression of numerous proteins required for proper DA synthesis and signaling is likely related to its ability to negatively regulate $G_{i/o}$-coupled $D_2$Rs present in SNc DA neurons. In support of this hypothesis, previous studies have shown that selective genetic ablation of $D_2$Rs within the mouse nigrostriatal pathway is associated with an increase in DA synthesis and release as well as increased locomotion (42). In addition, we previously showed (16) that $D_2$R expression was unaltered in SNc DA neurons lacking RGS6, despite altered expression of DAT and VMAT2, proteins regulated by the $D_2$R (37–40, 77–79). These findings suggest that altered $D_2$R signaling in the RGS6$^{-/-}$ mouse is likely due to loss of RGS6-mediated inhibition of $G_{i/o}$ protein signaling. In agreement with these findings, quinpirole suppression of locomotion, which is mediated exclusively by $D_2$Rs (42–45), is significantly greater in RGS6$^{-/-}$ than RGS6$^{+/+}$ mice (Figure 4). These data provide evidence that RGS6 regulates $D_2$R activity in the presynaptic terminal within the nigrostriatal pathway, not the striatal postsynaptic $D_2$Rs. Importantly, increased $D_2$R activity in RGS6$^{-/-}$ mice could explain the reduction in striatal DA seen in young mice (3 months; Figure 2).

Direct support of this possibility was provided by analysis of effects of RGS6 deficiency on pS40 TH levels in SNc DA neurons. It is well known that TH is activated by PKA-mediated phosphorylation on S40, known to be diminished by activation of presynaptic $D_2$Rs (43, 80). We showed that 12-month-old RGS6$^{-/-}$ mice exhibit a significant reduction in levels of pS40 TH, which was rescued by inhibiting presynaptic $D_2$Rs or by elevating cAMP to oppose $D_2$R-$G_{i/o}$–mediated suppression of cAMP. These findings show that RGS6 functions to negatively regulate $D_2$R-$G_{i/o}$ signaling in SNc DA neurons and support our behavioral studies in which RGS6$^{-/-}$ mice had significantly increased suppression of locomotion by quinpirole. Further, these results support our hypothesis that RGS6 may protect against PD pathogenesis through its ability to block $D_2$R-mediated inhibition of DA synthesis and signaling (Figure 7), an inhibition which can be neurotoxic. For example, cytosolic DA and its metabolites are neurotoxic (66, 69, 72) and increased expression of DAT provokes SNc neuronal cell death (71).

Together, our data portray a critical role for RGS6 in proper nigrostriatal DA synthesis and neurotransmission, required for normal motor control. Our data are consistent with several PD studies, including those using rodent models of neurochemical lesions (27, 28, 31, 32, 36), transgenic rodent models of PD (29, 30, 33–35), and studies of human patients with PD (81). Interestingly, both deficits in motor coordination and synchrony seen in RGS6$^{-/-}$ mice were partially reversed through L-DOPA treatment, but not through treatment with a $GABA_B$R antagonist (Figure 3). These data stand in contrast to our previous report that motor coordination deficits measured in 3-month-old RGS6$^{-/-}$ mice were related to disinhibition of the $GABA_B$R (26). Therefore, the results presented in this article conclusively demonstrate that RGS6 loss in aged animals leads to increased $D_2$R activity and reduced DA neurotransmission within the nigrostriatal pathway manifesting as a PD-associated impairment in motor performance. Interestingly, another R7 family member, RGS9, has also been implicated as a key regulator of nigrostriatal function (82–84). However, analysis of RGS9 expression reveals that instead of being expressed in SNc DA neurons, it is expressed and upregulated in striatal neurons during human PD (82). Similar to RGS6$^{-/-}$ mice, genetic ablation of RGS9-2 leads to increased striatal neuron $D_2$R activity and PD-like motor deficits (84–86). RGS6 loss had no effects on levels of expression of RGS9, which is expressed in striatum but not SNc, or other R7 family members in the SNc or striatum by Western blotting (Supplemental Figure 3).

The ability of RGS6 to promote cAMP-PKA signaling likely contributes to both its neuroprotective functions as well as its ability to suppress aberrant α-synuclein accumulation in the SNc. RGS6, through inhibition of $G_{i/o}$, is a predominant neuronal modulator of adenylyl cyclase activation and cAMP signaling (20, 21, 25, 26, 41). Our finding that RGS6 inhibits $G_{i/o}$-linked $D_2$R signaling in SNc DA neurons is significant, as cAMP-PKA signaling has been linked to SNc neuron survival and hence PD prevention. First, cAMP-elevating $\beta_2$ agonists reduce α-synuclein expression, decrease the risk of human PD, and protect against PD in mice and human cells (15). Second, inhibition of mitochondrial fission by PKA-mediated dynamin-related protein 1 phosphorylation is neuroprotective in mouse PD and cell culture models (53–55). In agreement with these previous reports, we observed elevated SNc α-synuclein protein expression in 12- and 18-month-old RGS6$^{-/-}$ mice relative to RGS6$^{+/+}$ controls. The aberrant elevation in α-synuclein expression in the SNc of RGS6$^{-/-}$ mice was accompanied by a transition in α-synuclein expression patterns from largely intracellular, as seen in RGS6$^{+/+}$ mice, to largely extracellular (Figure 5). These data may either reflect a change in α-synuclein handling in the SNc of RGS6$^{-/-}$ mice or the persistence of previously intracellular α-synuclein aggregates after DA neurons have degenerated. These data are intriguing, as the presence of extracellular α-synuclein aggregates has been well-documented in various PD models, and it has also been shown that these extracellular aggregates may play an important role in PD pathology, as they can be transmitted to other neurons, glia, and brain regions

(46–48). Together, our data provide evidence that RGS6 increases cAMP in SNc DA neurons to promote proper neuronal function/survival as well as suppress cytotoxic α-synuclein accumulation. It will be important to determine the role of α-synuclein in neurodegeneration in RGS6-deficient mice and to perform future rescue studies with viral expression of RGS6.

Based upon our findings, we propose that RGS6 protects against PD pathogenesis by suppressing the $D_2R$-$G_{i/o}$ signaling axis in SNc DA neurons, ensuring normal DA synthesis and release while preventing accumulation of cytotoxic DA metabolites and pathological α-synuclein (Figure 7). We believe this work positions RGS6 as a potentially novel avenue for therapeutic strategies in Parkinson's neurodegeneration.

## Methods

*Animals*. RGS6-knockout ($RGS6^{-/-}$) mice (129/Sv × C57BL6 background) were described previously (41). $RGS6^{-/-}$ mice were backcrossed 5–15 times with the C57BL/6J mouse strain. Three-, nine-, twelve-, and eighteen-month-old $RGS6^{+/+}$ and $RGS6^{-/-}$ mice of both sexes were used. Mice were housed with a continuous supply of food and water in a room maintained at 22°C, with a relative humidity of 20%–30% and a 12-hour/12-hour light/dark cycle. Behavioral studies were performed between 10 am and 4 pm.

*Neurochemical analysis*. $RGS6^{+/+}$ and $RGS6^{-/-}$ mice were euthanized at 3, 9, and 12 months of age. SNc and striatum were rapidly dissected and stored at –80°C. All samples were sent to the Vanderbilt Neurochemistry core for dopamine/metabolite extraction and HPLC analysis.

*Behavioral analyses*. All behavioral studies were performed using male mice. Behavioral analyses were performed in $RGS6^{+/+}$ and $RGS6^{-/-}$ animals that were (a) 12 months of age (model of age-onset PD) and received i.p. injections of saline, L-DOPA (25 mg/kg; Tocris Biosciences), or SCH-50911 (30 mg/kg: Tocris Biosciences) or (b) 3 months of age and injected with a quinpirole (300 μg/kg) assay of $D_2R$ function.

*Accelerating rotarod test*. The balance, motor coordination, and strength of mice were assessed using a motorized rotarod apparatus (Ugo Basile). For this test, mice underwent 2 consecutive days of training in which they were placed on a motorized rotarod that increased rotation speed from 4 to 40 rpm over a 5-minute period. For each training day, mice were provided 3 opportunities to maintain their perch on the rotarod as its speed increased. On the third day, the time it took the mice to fall from the beam was recorded. For this analysis, the 12-month-old $RGS6^{+/+}$ and $RGS6^{-/-}$ mice were injected i.p. with saline, L-DOPA (25 mg/kg), or the $GABA_B$ receptor antagonist SCH-50911 (30 mg/kg) 20 minutes prior to testing.

*Open-field test*. Locomotor activity was assessed using an open-field test. For this test, mice were placed in an open-field box and were video recorded from above as they explored this novel environment for 10 minutes. The total distance traveled by each mouse was measured using these video recordings. To evaluate quinpirole suppression of locomotion, locomotor activity was measured for 15 minutes following i.p. injection with saline or quinpirole (300 μg/kg). EthoVision TX 11.5 software recorded the video and scored automatically for locomotor parameters.

*DigiGait analysis*. An automated treadmill gait analysis was performed using the DigiGait Imaging System (Mouse Specifics Inc.; refs. 26, 28). For this analysis, mice were placed on a treadmill that was set at a fixed belt speed of 15 cm/s (a speed at which all aged animals were able to walk) and were video recorded using a camera mounted underneath the treadmill belt. The video recording was automatically processed by the DigiGait Imaging System software to calculate standard gait parameters. This test was used to analyze the gait of 12-month-old $RGS6^{+/+}$ and $RGS6^{-/-}$ mice that received i.p. injections of either saline, L-DOPA (25 mg/kg), or the $GABA_BR$ antagonist SCH-50911 (30 mg/kg) 20 minutes prior to testing.

*Immunohistochemistry*. IHC analysis of RGS6 and TH expression was performed in both human and mouse SNc tissues. For these analyses, both human control and PD SNc containing midbrain sections were supplied by the Harvard Brain Tissue Resource Center via NIH NeuroBioBank Brain and Tissue Repositories. In preparation for the IHC analysis, mouse brain tissues were harvested from mice perfused with ice-cold saline followed by 4% paraformaldehyde. The whole brain was harvested and postfixed in 4% paraformaldehyde at 4°C overnight before being sunk in a 30% sucrose solution. Ten-micrometer coronal sections containing SNc were collected. Both human and mouse SNc tissue sections were placed in blocking/extraction solution (0.5% Triton X-100 and 10% goat serum in 1× PBS) for 1 hour at room temperature. After blocking, tissues were incubated overnight at 4°C in rabbit anti-RGS6 (homemade polyclonal antibody against the entire RGS6 protein 1:100, ref. 26) or mouse anti-TH (1:100; Millipore, MAB318). Additional IHC analysis of α-synuclein, phospho-PKA substrate, and pS40 TH was performed in mouse SNc tissues prepared as described previously using rabbit phospho-PKA substrate (1:100; Cell Signaling, 9621S), phosphoS40 TH (1:100; Cell Signaling, 2791S), and rabbit anti–α-synuclein (1:100; MilliporeSigma, S3062) primary antibody diluted in blocking/extraction solution. After washing with room temperature once with PBS, tissues were incubated in Alexa Fluor 488/647–conjugated secondary antibodies (Life Technologies, A11029/A21245; 1:2,000/1,000) in blocking solution for 1 hour at room temperature. Fluorescently stained tissue slices were imaged using a Zeiss 710 confocal microscope as previously described (87).

*Unbiased stereological analysis of cell numbers*. Quantification of RGS6- and TH-stained cells in human control and PD SNc sections was performed using unbiased stereological analysis using the Zeiss Axioskope 2 Mot Plus (Carl Zeiss) attached to a motorized stage and connected to a computer running the stereo Investigator software (MicroBrightfield) as previously described (88). In brief, RGS6- and TH-stained cells were counted using the optical fractionator probe with a ×40 oil-immersion objective. Sampling grids sized 1,200 μm × 1,200 μm with a counting frame of 300 μm × 300 μm were used for human samples and 150-μm × 150-μm sampling grids with a counting frame of 50 μm × 50 μm were used for mice. The StereoInvestigator was automatically placed at each intersection point. Serial coronal sections (one every 200 μm) were used for the counts.

*ImageJ quantification of α-synuclein, phospho-PKA substrate, and pS40 TH*. Quantification of α-synuclein, phospho-PKA substrate, and pS40 TH was performed using ImageJ software (NIH). Images were converted to grayscale and total fluorescence of the field (α-synuclein) was measured. The area, integrated density, and mean background fluorescence recordings were used to calculate the corrected total fluorescence of the field. Corrected total fluorescence was calculated according to the ImageJ user manual and was obtained by subtracting the product of the area and the mean background fluorescence from the integrated density. The percentage of $TH^+$ neurons with intracellular α-synuclein or phospho-PKA substrate and the levels of pS40 TH in SNc DA neurons were also measured. Data are presented as mean ± SEM corrected total fluorescence.

*Immunoblotting*. Frozen SNc samples were placed in RIPA lysis buffer (150 mM NaCl, 1.0% NP-40, 0.5% sodium deoxycholate, 0.1% SDS, 50 mM Tris-HCL [pH 8.0]) containing protease and phosphatase inhibitors (MilliporeSigma, P8340/P5726). Tissues were homogenized using a Dounce homogenizer and centrifuged at 14,000 *g* for 10 minutes (4°C) to isolate the protein-rich supernatant. This supernatant was combined with Laemmli buffer, boiled for 5 minutes, and loaded onto a 4% to 20% SDS/PAGE gel. Following transfer, blots were probed with rabbit anti-RGS6 (homemade polyclonal antibody against the entire RGS6 protein; 1:2000), mouse anti–α-synuclein (1:500; BD Biosciences, 610787), rabbit anti-GAPDH (1:1000; MilliporeSigma, G9545) primary antibodies, and Alexa Fluor 800–conjugated goat anti-rabbit (LI-COR Biosciences 680RD) or goat anti-mouse (LI-COR Biosciences 800CW) secondary antibodies. Immunoblots were visualized using the Odyssey Imaging System. In other experiments, frozen SNc and striatum samples from $RGS6^{+/+}$ and $RGS6^{–/–}$ mice were prepared as described previously and probed with rabbit anti-RGS6 (as above), anti-RGS7 (a gift from Vladlen Z. Slepak, University of Miami, Miami, Florida, USA, 1:1000 dilution), anti-RGS9-2 (a gift from Steve Gold, UT Southwestern, Dallas, Texas, USA, 1:1000 dilution), and anti-RGS11 (a gift from Jason Chen, Baylor, Houston, Texas, USA, 1:1000 dilution).

*Statistics*. Data are expressed as mean ± SEM. One- or two-way ANOVAs with the Fisher least significant difference (LSD) post hoc adjustment were used for data analysis. $P < 0.05$ was considered statistically significant. Statistical analyses were performed using XLSTAT software.

*Study approval*. All procedures were approved and performed in accordance with guidelines provided by the Institutional Animal Care and Use Committee at the University of Iowa.

## Author contributions

RAF acquired funding for the study. ZL, KEAD, NSN, and RAF designed the study. KEAD, JY, and RAF supervised the study. JY, SA, HES, and NSN provided resources for the study. ZL, KEAD, MMS, JY, SA, HES, NSN, and RAF developed study methodology. ZL, KEAD, JY, and MMS performed experiments. MMS and HES performed statistical analyses. ZL prepared the original draft of the manuscript. KEAD, NSN, and RAF helped write the manuscript and KEAD, RAF, MMS, and JY reviewed/edited the manuscript before submission.

## Acknowledgments

The work presented in this manuscript was supported by NIH grants AA025919, NS098687, and CA161882; the Michael J. Fox Foundation (11551); the Iowa Cardiovascular Interdisciplinary Research Fellowship (T32HL007121); and Iowa Pharmacological Sciences (T32GM067795). The content is solely the responsibility of the authors and does not necessarily represent the official views of the National Institutes of Health. The authors thank the NIH NeuroBioBank for providing PD and control human midbrain specimens. The authors also thank Michael J. Welsh (University of Iowa) for careful reading of and useful suggestions for this manuscript.

Address correspondence to: Rory A. Fisher, Department of Pharmacology, University of Iowa, Carver College of Medicine, 51 Newton Road, BSB 2-512, Iowa City, Iowa 52242, USA. Phone: 319.335.8330; Email: rory-fisher@uiowa.edu.

---

1. Nussbaum RL, Ellis CE. Alzheimer's disease and Parkinson's disease. *N Engl J Med*. 2003;348(14):1356–1364.
2. Fahn S. The history of dopamine and levodopa in the treatment of Parkinson's disease. *Mov Disord*. 2008;23(suppl 3):S497–S508.
3. Meissner WG, et al. Priorities in Parkinson's disease research. *Nat Rev Drug Discov*. 2011;10(5):377–393.
4. Shulman JM, De Jager PL, Feany MB. Parkinson's disease: genetics and pathogenesis. *Annu Rev Pathol*. 2011;6:193–222.
5. Fearnley JM, Lees AJ. Ageing and Parkinson's disease: substantia nigra regional selectivity. *Brain*. 1991;114 (pt 5):2283–2301.
6. Kim HJ. α-Synuclein expression in patients with Parkinson's disease: a clinician's perspective. *Exp Neurobiol*. 2013;22(2):77–83.
7. Chartier-Harlin MC, et al. α-Synuclein locus duplication as a cause of familial Parkinson's disease. *Lancet*. 2004;364(9440):1167–1169.
8. Singleton AB, et al. α-Synuclein locus triplication causes Parkinson's disease. *Science*. 2003;302(5646):841.
9. Stefanis L. α-Synuclein in Parkinson's disease. *Cold Spring Harb Perspect Med*. 2012;2(2):a009399.
10. Chu Y, Kordower JH. Age-associated increases of alpha-synuclein in monkeys and humans are associated with nigrostriatal dopamine depletion: is this the target for Parkinson's disease? *Neurobiol Dis*. 2007;25(1):134–149.
11. Li W, Lesuisse C, Xu Y, Troncoso JC, Price DL, Lee MK. Stabilization of α-synuclein protein with aging and familial Parkinson's disease-linked A53T mutation. *J Neurosci*. 2004;24(33):7400–7409.
12. Giasson BI, Duda JE, Quinn SM, Zhang B, Trojanowski JQ, Lee VM. Neuronal α-synucleinopathy with severe movement disorder in mice expressing A53T human α-synuclein. *Neuron*. 2002;34(4):521–533.
13. Masliah E, et al. Dopaminergic loss and inclusion body formation in α-synuclein mice: implications for neurodegenerative disorders. *Science*. 2000;287(5456):1265–1269.
14. Luk KC, Kehm VM, Zhang B, O'Brien P, Trojanowski JQ, Lee VM. Intracerebral inoculation of pathological α-synuclein initiates a rapidly progressive neurodegenerative α-synucleinopathy in mice. *J Exp Med*. 2012;209(5):975–986.
15. Mittal S, et al. β2-Adrenoreceptor is a regulator of the α-synuclein gene driving risk of Parkinson's disease. *Science*. 2017;357(6354):891–898.
16. Bifsha P, Yang J, Fisher RA, Drouin J. Rgs6 is required for adult maintenance of dopaminergic neurons in the ventral substantia nigra. *PLoS Genet*. 2014;10(12):e1004863.
17. Berman DM, Wilkie TM, Gilman AG. GAIP and RGS4 are GTPase-activating proteins for the Gi subfamily of G protein α subunits. *Cell*. 1996;86(3):445–452.
18. Hepler JR, Berman DM, Gilman AG, Kozasa T. RGS4 and GAIP are GTPase-activating proteins for Gq α and block activation of phospholipase C beta by gamma-thio-GTP-Gq α. *Proc Natl Acad Sci U S A*. 1997;94(2):428–432.
19. Ross EM, Wilkie TM. GTPase-activating proteins for heterotrimeric G proteins: regulators of G protein signaling (RGS) and RGS-like proteins. *Annu Rev Biochem*. 2000;69:795–827.
20. Posner BA, Gilman AG, Harris BA. Regulators of G protein signaling 6 and 7. Purification of complexes with gβ5 and assessment of their effects on g protein-mediated signaling pathways. *J Biol Chem*. 1999;274(43):31087–31093.
21. Hooks SB, Waldo GL, Corbitt J, Bodor ET, Krumins AM, Harden TK. RGS6, RGS7, RGS9, and RGS11 stimulate GTPase activity of Gi family G-proteins with differential selectivity and maximal activity. *J Biol Chem*. 2003;278(12):10087–10093.
22. Damier P, Hirsch EC, Agid Y, Graybiel AM. The substantia nigra of the human brain. I. Nigrosomes and the nigral matrix, a compartmental organization based on calbindin D(28K) immunohistochemistry. *Brain*. 1999;122(pt 8):1421–1436.
23. Karoum F, Neff NH, Wyatt RJ. The dynamics of dopamine metabolism in various regions of rat brain. *Eur J Pharmacol*. 1977;44(4):311–318.
24. Pifl C, et al. Is Parkinson's disease a vesicular dopamine storage disorder? Evidence from a study in isolated synaptic vesicles of human and nonhuman primate striatum. *J Neurosci*. 2014;34(24):8210–8218.
25. Stewart A, et al. Regulator of G-protein signaling 6 (RGS6) promotes anxiety and depression by attenuating serotonin-mediated activation of the 5-HT(1A) receptor-adenylyl cyclase axis. *FASEB J*. 2014;28(4):1735–1744.
26. Maity B, et al. Regulator of G protein signaling 6 (RGS6) protein ensures coordination of motor movement by modulating GABAB receptor signaling. *J Biol Chem*. 2012;287(7):4972–4981.
27. Tillerson JL, Caudle WM, Reverón ME, Miller GW. Detection of behavioral impairments correlated to neurochemical deficits in mice treated with moderate doses of 1-methyl-4-phenyl-1,2,3,6-tetrahydropyridine. *Exp Neurol*. 2002;178(1):80–90.
28. Amende I, Kale A, McCue S, Glazier S, Morgan JP, Hampton TG. Gait dynamics in mouse models of Parkinson's disease and Huntington's disease. *J Neuroeng Rehabil*. 2005;2:20.
29. Goldberg MS, et al. Nigrostriatal dopaminergic deficits and hypokinesia caused by inactivation of the familial Parkinsonism-linked gene DJ-1. *Neuron*. 2005;45(4):489–496.
30. Gispert S, et al. Parkinson phenotype in aged PINK1-deficient mice is accompanied by progressive mitochondrial dysfunction in absence of neurodegeneration. *PLoS One*. 2009;4(6):e5777.
31. Glajch KE, Fleming SM, Surmeier DJ, Osten P. Sensorimotor assessment of the unilateral 6-hydroxydopamine mouse model of Parkinson's disease. *Behav Brain Res*. 2012;230(2):309–316.
32. Carvalho MM, et al. Behavioral characterization of the 6-hydroxidopamine model of Parkinson's disease and pharmacological rescuing of non-motor deficits. *Mol Neurodegener*. 2013;8:14.
33. Janezic S, et al. Deficits in dopaminergic transmission precede neuron loss and dysfunction in a new Parkinson model. *Proc Natl*

*Acad Sci U S A*. 2013;110(42):E4016–E4025.
34. Lieu CA, Chinta SJ, Rane A, Andersen JK. Age-related behavioral phenotype of an astrocytic monoamine oxidase-B transgenic mouse model of Parkinson's disease. *PLoS One*. 2013;8(1):e54200.
35. Blesa J, Przedborski S. Parkinson's disease: animal models and dopaminergic cell vulnerability. *Front Neuroanat*. 2014;8:155.
36. Zhou M, et al. Gait analysis in three different 6-hydroxydopamine rat models of Parkinson's disease. *Neurosci Lett*. 2015;584:184–189.
37. Adell A, Artigas F. The somatodendritic release of dopamine in the ventral tegmental area and its regulation by afferent transmitter systems. *Neurosci Biobehav Rev*. 2004;28(4):415–431.
38. Chen R, et al. Protein kinase Cβ is a modulator of the dopamine D2 autoreceptor-activated trafficking of the dopamine transporter. *J Neurochem*. 2013;125(5):663–672.
39. Dickinson SD, et al. Dopamine D2 receptor-deficient mice exhibit decreased dopamine transporter function but no changes in dopamine release in dorsal striatum. *J Neurochem*. 1999;72(1):148–156.
40. Ford CP. The role of D2-autoreceptors in regulating dopamine neuron activity and transmission. *Neuroscience*. 2014;282:13–22.
41. Yang J, et al. RGS6, a modulator of parasympathetic activation in heart. *Circ Res*. 2010;107(11):1345–1349.
42. Bello EP, et al. Cocaine supersensitivity and enhanced motivation for reward in mice lacking dopamine D2 autoreceptors. *Nat Neurosci*. 2011;14(8):1033–1038.
43. Lindgren N, et al. Distinct roles of dopamine D2L and D2S receptor isoforms in the regulation of protein phosphorylation at presynaptic and postsynaptic sites. *Proc Natl Acad Sci U S A*. 2003;100(7):4305–4309.
44. Usiello A, et al. Distinct functions of the two isoforms of dopamine D2 receptors. *Nature*. 2000;408(6809):199–203.
45. Wang Y, Xu R, Sasaoka T, Tonegawa S, Kung MP, Sankoorikal EB. Dopamine D2 long receptor-deficient mice display alterations in striatum-dependent functions. *J Neurosci*. 2000;20(22):8305–8314.
46. Lashuel HA, Overk CR, Oueslati A, Masliah E. The many faces of α-synuclein: from structure and toxicity to therapeutic target. *Nat Rev Neurosci*. 2013;14(1):38–48.
47. Ottolini D, Calí T, Szabò I, Brini M. Alpha-synuclein at the intracellular and the extracellular side: functional and dysfunctional implications. *Biol Chem*. 2017;398(1):77–100.
48. Lee HJ, Bae EJ, Lee SJ. Extracellular α-synuclein-a novel and crucial factor in Lewy body diseases. *Nat Rev Neurol*. 2014;10(2):92–98.
49. Lee MK, et al. Human alpha-synuclein-harboring familial Parkinson's disease-linked Ala-53 --> Thr mutation causes neurodegenerative disease with alpha-synuclein aggregation in transgenic mice. *Proc Natl Acad Sci U S A*. 2002;99(13):8968–8973.
50. Tofaris GK, et al. Pathological changes in dopaminergic nerve cells of the substantia nigra and olfactory bulb in mice transgenic for truncated human alpha-synuclein (1-120): implications for Lewy body disorders. *J Neurosci*. 2006;26(15):3942–3950.
51. Kahle PJ, et al. Subcellular localization of wild-type and Parkinson's disease-associated mutant alpha-synuclein in human and transgenic mouse brain. *J Neurosci*. 2000;20(17):6365–6373.
52. Giaime E, Tong Y, Wagner LK, Yuan Y, Huang G, Shen J. Age-dependent dopaminergic neurodegeneration and impairment of the autophagy-lysosomal pathway in LRRK-deficient mice. *Neuron*. 2017;96(4):796–807.e6.
53. Dagda RK, et al. Mitochondrially localized PKA reverses mitochondrial pathology and dysfunction in a cellular model of Parkinson's disease. *Cell Death Differ*. 2011;18(12):1914–1923.
54. Rappold PM, et al. Drp1 inhibition attenuates neurotoxicity and dopamine release deficits in vivo. *Nat Commun*. 2014;5:5244.
55. Wang X, et al. DLP1-dependent mitochondrial fragmentation mediates 1-methyl-4-phenylpyridinium toxicity in neurons: implications for Parkinson's disease. *Aging Cell*. 2011;10(5):807–823.
56. Duty S, Jenner P. Animal models of Parkinson's disease: a source of novel treatments and clues to the cause of the disease. *Br J Pharmacol*. 2011;164(4):1357–1391.
57. Tieu K. A guide to neurotoxic animal models of Parkinson's disease. *Cold Spring Harb Perspect Med*. 2011;1(1):a009316.
58. Snow BE, Betts L, Mangion J, Sondek J, Siderovski DP. Fidelity of G protein beta-subunit association by the G protein gamma-subunit-like domains of RGS6, RGS7, and RGS11. *Proc Natl Acad Sci U S A*. 1999;96(11):6489–6494.
59. Witherow DS, et al. Complexes of the G protein subunit gbeta 5 with the regulators of G protein signaling RGS7 and RGS9. Characterization in native tissues and in transfected cells. *J Biol Chem*. 2000;275(32):24872–24880.
60. Xie K, et al. Gβ5-RGS complexes are gatekeepers of hyperactivity involved in control of multiple neurotransmitter systems. *Psychopharmacology (Berl)*. 2012;219(3):823–834.
61. Vaughan RA, Foster JD. Mechanisms of dopamine transporter regulation in normal and disease states. *Trends Pharmacol Sci*. 2013;34(9):489–496.
62. Bernheimer H, Birkmayer W, Hornykiewicz O, Jellinger K, Seitelberger F. Brain dopamine and the syndromes of Parkinson and Huntington. Clinical, morphological and neurochemical correlations. *J Neurol Sci*. 1973;20(4):415–455.
63. Hefti F, Enz A, Melamed E. Partial lesions of the nigrostriatal pathway in the rat. Acceleration of transmitter synthesis and release of surviving dopaminergic neurones by drugs. *Neuropharmacology*. 1985;24(1):19–23.
64. Bezard E, et al. Relationship between the appearance of symptoms and the level of nigrostriatal degeneration in a progressive 1-methyl-4-phenyl-1,2,3,6-tetrahydropyridine-lesioned macaque model of Parkinson's disease. *J Neurosci*. 2001;21(17):6853–6861.
65. Tokuoka H, et al. Compensatory regulation of dopamine after ablation of the tyrosine hydroxylase gene in the nigrostriatal projection. *J Biol Chem*. 2011;286(50):43549–43558.
66. Mosharov EV, et al. Interplay between cytosolic dopamine, calcium, and alpha-synuclein causes selective death of substantia nigra neurons. *Neuron*. 2009;62(2):218–229.
67. Jacobs FM, et al. Retinoic acid-dependent and -independent gene-regulatory pathways of Pitx3 in meso-diencephalic dopaminergic neurons. *Development*. 2011;138(23):5213–5222.
68. Cai H, Liu G, Sun L, Ding J. Aldehyde dehydrogenase 1 making molecular inroads into the differential vulnerability of nigrostriatal dopaminergic neuron subtypes in Parkinson's disease. *Transl Neurodegener*. 2014;3:27.
69. Liu G, et al. Aldehyde dehydrogenase 1 defines and protects a nigrostriatal dopaminergic neuron subpopulation. *J Clin Invest*. 2014;124(7):3032–3046.

70. Lohr KM, et al. Increased vesicular monoamine transporter enhances dopamine release and opposes Parkinson disease-related neurodegeneration in vivo. *Proc Natl Acad Sci U S A*. 2014;111(27):9977–9982.
71. Masoud ST, et al. Increased expression of the dopamine transporter leads to loss of dopamine neurons, oxidative stress and l-DOPA reversible motor deficits. *Neurobiol Dis*. 2015;74:66–75.
72. Caudle WM, et al. Reduced vesicular storage of dopamine causes progressive nigrostriatal neurodegeneration. *J Neurosci*. 2007;27(30):8138–8148.
73. Vergo S, Johansen JL, Leist M, Lotharius J. Vesicular monoamine transporter 2 regulates the sensitivity of rat dopaminergic neurons to disturbed cytosolic dopamine levels. *Brain Res*. 2007;1185:18–32.
74. Afonso-Oramas D, et al. Dopamine transporter glycosylation correlates with the vulnerability of midbrain dopaminergic cells in Parkinson's disease. *Neurobiol Dis*. 2009;36(3):494–508.
75. González-Hernández T, Cruz-Muros I, Afonso-Oramas D, Salas-Hernandez J, Castro-Hernandez J. Vulnerability of mesostriatal dopaminergic neurons in Parkinson's disease. *Front Neuroanat*. 2010;4:140.
76. Lipski J, Nistico R, Berretta N, Guatteo E, Bernardi G, Mercuri NB. L-DOPA: a scapegoat for accelerated neurodegeneration in Parkinson's disease? *Prog Neurobiol*. 2011;94(4):389–407.
77. Mayfield RD, Zahniser NR. Dopamine D2 receptor regulation of the dopamine transporter expressed in Xenopus laevis oocytes is voltage-independent. *Mol Pharmacol*. 2001;59(1):113–121.
78. Höltje M, et al. The neuronal monoamine transporter VMAT2 is regulated by the trimeric GTPase Go(2). *J Neurosci*. 2000;20(6):2131–2141.
79. Bolan EA, et al. D2 receptors regulate dopamine transporter function via an extracellular signal-regulated kinases 1 and 2-dependent and phosphoinositide 3 kinase-independent mechanism. Mol Pharmacol. 2007;71(5):1222–1232.
80. Lindgren N, Xu ZQ, Herrera-Marschitz M, Haycock J, Hökfelt T, Fisone G. Dopamine D(2) receptors regulate tyrosine hydroxylase activity and phosphorylation at Ser40 in rat striatum. *Eur J Neurosci*. 2001;13(4):773–780.
81. Lewis GN, Byblow WD, Walt SE. Stride length regulation in Parkinson's disease: the use of extrinsic, visual cues. *Brain*. 2000;123(pt 10):2077–2090.
82. Tekumalla PK, et al. Elevated levels of DeltaFosB and RGS9 in striatum in Parkinson's disease. *Biol Psychiatry*. 2001;50(10):813–816.
83. Rahman Z, et al. RGS9 modulates dopamine signaling in the basal ganglia. *Neuron*. 2003;38(6):941–952.
84. Gold SJ, et al. RGS9-2 negatively modulates L-3,4-dihydroxyphenylalanine-induced dyskinesia in experimental Parkinson's disease. *J Neurosci*. 2007;27(52):14338–14348.
85. Kovoor A, et al. D2 dopamine receptors colocalize regulator of G-protein signaling 9-2 (RGS9-2) via the RGS9 DEP domain, and RGS9 knock-out mice develop dyskinesias associated with dopamine pathways. *J Neurosci*. 2005;25(8):2157–2165.
86. Celver J, Sharma M, Kovoor A. RGS9-2 mediates specific inhibition of agonist-induced internalization of D2-dopamine receptors. *J Neurochem*. 2010;114(3):739–749.
87. Stewart A, Maity B, Anderegg SP, Allamargot C, Yang J, Fisher RA. Regulator of G protein signaling 6 is a critical mediator of both reward-related behavioral and pathological responses to alcohol. *Proc Natl Acad Sci U S A*. 2015;112(7):E786–E795.
88. Salmaso N, et al. Fibroblast growth factor 2 modulates hypothalamic pituitary axis activity and anxiety behavior through glucocorticoid receptors. *Biol Psychiatry*. 2016;80(6):479–489.